iScience

CellPress
OPEN ACCESS

Article

# A heterozygous *ZP2* mutation causes zona pellucida defects and female infertility in mouse and human

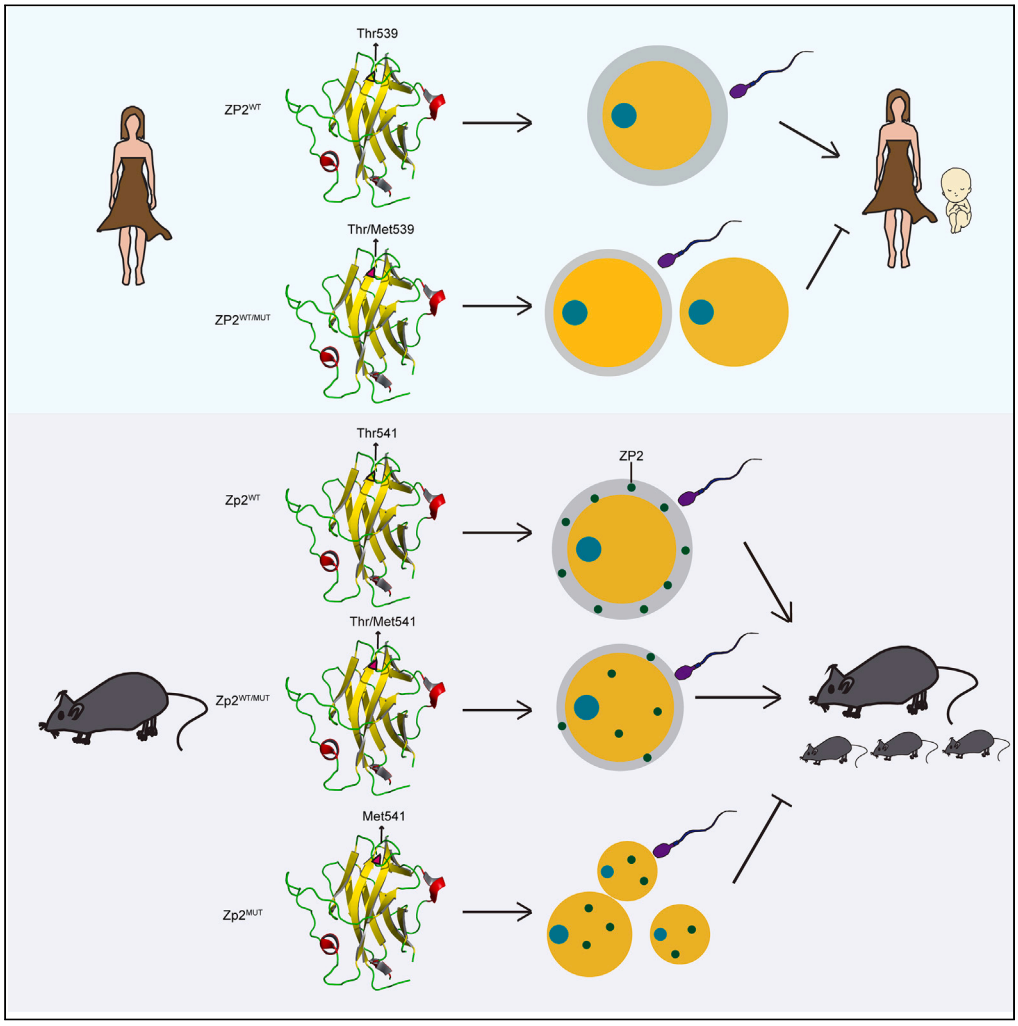


Sai-Li Liu, Hai-Yang Zuo, Bing-Wang Zhao, ..., Wei-Zhou Wang, Qing-Yuan Sun, Zhen-Bo Wang

wangweizhou12@126.com (W.-Z.W.)
sunqy@gd2h.org.cn (Q.-Y.S.)
wangzb@ioz.ac.cn (Z.-B.W.)

## Highlights

A novel heterozygous mutation of *ZP2* was identified in the primary infertile female

The mutation reduced ZP2 expression and impeded ZP2 secretion

Homozygous mutant ($Zp2^{T541M}$) mice recapitulated the female infertility phenotype

$Zp2^{T541M}$ mice exhibited impaired folliculogenesis and degenerated ZP-free oocytes

Liu et al., iScience *26*, 107828
October 20, 2023 © 2023 The Authors.
https://doi.org/10.1016/j.isci.2023.107828

iScience

CellPress
OPEN ACCESS

Article

# A heterozygous *ZP2* mutation causes zona pellucida defects and female infertility in mouse and human

Sai-Li Liu,[1,2] Hai-Yang Zuo,[3] Bing-Wang Zhao,[1,2] Jia-Ni Guo,[1,2] Wen-Bo Liu,[1] Wen-Long Lei,[1] Yuan-Yuan Li,[1] Ying-Chun Ouyang,[1] Yi Hou,[1] Zhi-Ming Han,[1,2,4,5] Wei-Zhou Wang,[3,*] Qing-Yuan Sun,[6,*] and Zhen-Bo Wang[1,2,4,5,7,*]

## SUMMARY

**The zona pellucida (ZP) is an extracellular glycoprotein matrix surrounding mammalian oocytes. Recently, numerous mutations in genes encoding ZP proteins have been shown to be possibly related to oocyte abnormality and female infertility; few reports have confirmed the functions of these mutations in living animal models. Here, we identified a novel heterozygous missense mutation (NM_001376231.1:c.1616C>T, p.Thr539Met) in *ZP2* from a primary infertile female. We showed that the mutation reduced ZP2 expression and impeded ZP2 secretion in cell lines. Furthermore, we constructed the mouse model with the mutation ($Zp2^{T541M}$) using CRISPR-Cas9. $Zp2^{WT/T541M}$ female mice had normal fertility though generated oocytes with the thin ZP, whereas $Zp2^{T541M}$ female mice were completely infertile due to degeneration of oocytes without ZP. Additionally, ZP deletion impaired folliculogenesis and caused female infertility in $Zp2^{T541M}$ mice. Our study not only expands the spectrum of *ZP2* mutation sites but also, more importantly, increases the understanding of pathogenic mechanisms of *ZP2* mutations.**

## INTRODUCTION

High-quality eggs in mammals are essential for successful fertilization and embryo development. For mammalian females, zona pellucida (ZP) is an extracellular matrix surrounding the oocyte. The ZP first appears around mouse oocytes in primary follicles and gradually thickens during oocyte growth, reaching its maximum thickness in fully grown oocytes.[1] The ZP serves essentially functional roles in oogenesis,[2,3] egg-sperm recognition and polyspermy avoidance during fertilization,[4–6] and safeguarding of preimplantation embryos.[1,7,8]

The ZP of human and most murine species consists of four glycosylated proteins called ZP1-ZP4;[9,10] whereas mouse ZP is composed of ZP1-ZP3 proteins, as *Zp4* is a pseudogene in mice.[10] Zona pellucida proteins are highly conserved and share some common structural motifs including signal peptide (SP), ZP domain (ZPD), consensus furin cleavage site (CFCS), internal hydrophobic peptide (IHP), external hydrophobic peptide (EHP), and transmembrane domain (TMD). The N-terminal SP is a hydrophobic sequence of 20–30 amino acids that sorts proteins into secretory pathway.[11] ZPD consists of 260 amino acids and contains ZP-C and ZP-N subdomains, which play a crucial role in zona pellucida protein-protein interactions and ZP polymerization.[12,13] CFCS is an Arg-X-X/Arg/Lys-Arg conserved sequence where proprotein convertase cleaves proteins.[1] EHP and IHP interact to remain zona pellucida proteins in monomeric state to prevent premature intracellular polymerization.[14,15] Downstream of EHP, TMD anchors the nascent zona pellucida proteins to secretory vesicles and plasma membrane.[16] TMD is required for CFCS cleavage and incorporation of nascent zona pellucida into the ZP.[14]

In mice, homozygous null for either *Zp2* ($Zp2^{-/-}$) or *Zp3* ($Zp3^{-/-}$) females was exclusively sterile, with smaller ovaries, and ovulated ZP-free eggs.[17,18] This evidence suggested that ZP2 and ZP3 were essential for the structure of ZP and for female reproduction. Homozygous null for *Zp1* ($Zp1^{-/-}$) female mice was less deficient than $Zp2^{-/-}$ and $Zp3^{-/-}$ female mice. Thin ZP composed of ZP2 and ZP3 was poorly organized and fragile, contributing to early embryonic loss and subfertility for $Zp1^{-/-}$ females.[19] In human, multiple mutations in *ZP1-ZP4* have so far been identified in association with female infertility.[20–23] Recent reviews summarized the mutations about the zona pellucida genes.[24,25] Among them, most of the *ZP2* mutations were identified to locate in ZPD, and the genotypes were mainly homozygous.[23,26–28] A homozygous variant of *ZP2* (c.1691_1694dup, p.Cys566Trpfs*5) located in ZP-C subdomain expressed a truncated ZP2 protein which resulted in thin ZP with irregularly arranged fibers and failure of *in vitro* fertilization (IVF).[26] Fortunately, the patient had a successful singleton pregnancy by

[1]State Key Laboratory of Stem Cell and Reproductive Biology, Institute of Zoology, Chinese Academy of Sciences, Beijing 100101, China
[2]University of Chinese Academy of Sciences, Beijing 101408, China
[3]The Six Medical Center of Chinese People's Liberation Army General Hospital, Beijing 100048, China
[4]Institute for Stem Cell and Regeneration, Chinese Academy of Sciences, Beijing 100101, China
[5]Beijing Institute for Stem Cell and Regenerative Medicine, Beijing 100101, China
[6]Guangzhou Key Laboratory of Metabolic Diseases and Reproductive Health, Guangdong-Hong Kong Metabolism & Reproduction Joint Laboratory, Reproductive Medicine Center, Guangdong Second Provincial General Hospital, Guangzhou 510317, China
[7]Lead contact
*Correspondence: wangweizhou12@126.com (W.-Z.W.), sunqy@gd2h.org.cn (Q.-Y.S.), wangzb@ioz.ac.cn (Z.-B.W.)
https://doi.org/10.1016/j.isci.2023.107828


This is an open access article under the CC BY-NC-ND license (http://creativecommons.org/licenses/by-nc-nd/4.0/).

**Table 1. The basic characteristics of IVF/ICSI attempts for the patient**

| Cycle | Protocol | Number of retrieved oocytes | MII oocytes | Abnormal oocytes | Immature oocytes | Fertilized oocytes | Available embryos |
|---|---|---|---|---|---|---|---|
| 1 | Mild stimulation | 24 | 5 | 15 | 4 | 2 | 2 |
| 2 | Mild stimulation | 17 | 5 | 11 | 1 | 2 | 1 |
| 3 | Long OC | 23 | 14 | 8 | 1 | 7 | 2 |

OC, oral contraceptive.

intracytoplasmic sperm injection (ICSI). Another study identified a ZP2 heterozygous mutation (c.1115G > C, p.Cys372Ser) from an infertile patient with thin and weak oocytes zona pellucida and poor-quality embryos obtained by IVF.[23] Two ZP2 heterozygous mutations (c.1599G>T, p.R533S; c.1696T>C, p.C566R) may be responsible for abnormal oocyte morphology (e.g., naked oocytes without ZP, a crackled ZP, oocytes degeneration, abnormal ZP, and perivitelline space) in patients.[27] Although increasing reports showed the possible correlation between various mutations of genes encoding ZP protein with female infertility, few confirmed gene mutations functions by animal models.

Here, we identified a novel *ZP2* heterozygous mutation (NM_001376231.1: c.1616C>T, p.Thr539Met) from an infertile female with abnormal ZP oocytes. Cell lines and mouse model were used to investigate the effects of the mutation on ZP formation and female reproduction. We found that the heterozygous mutation interfered with ZP2 secretion, resulting in a thin ZP but normal fertility in $Zp2^{WT/T541M}$ female mice. Homozygous mutation compromised ZP2 expression and secretion, causing aberrant intracellular localization of ZP2 and failure of ZP formation. Meanwhile, $Zp2^{T541M}$ homozygous mutation impaired follicular development and reduced the number of tertiary follicles, which led to oocyte degeneration and lower ovulation, and ultimately caused female infertility.

## RESULTS

### Clinical description of the patient

The proband (family member II-2) was a 37-year-old woman who had not conceived through unprotected sexual intercourse, with a diagnosis of primary infertility for 4 years. Her chromosome karyotype was 46, XX and basal sex hormone levels were as follows. The follicle-stimulating hormone level was 3.4 IU/L, luteinizing hormone level was 1.1 IU/L, prolactin level was 7.6 ng/mL, estradiol level was 28 pg/mL, and testosterone level was below 20 ng/mL. The image of hysterosalpingography showed that her right fallopian tube was obstructed and the left side had poor diffusion. Her husband was 37 years old with normal karyotype and semen analysis. Following two previous unsuccessful IVF treatments elsewhere, she underwent three IVF/ICSI cycles at the Sixth Medical Center for Chinese People's Liberation Army General Hospital (Table 1). In the first IVF cycle, 24 cumulus-oocyte complexes (COCs)/oocytes were obtained, containing 5 ZP-thin metaphase-II (MII) oocytes, 4 immature metaphase-I oocytes, and 15 abnormal oocytes which were ZP free and naked ZP without oocytes. Five MII oocytes underwent conventional *in vitro* fertilization and two MII oocytes were successfully fertilized and developed into 8-cell embryos which had been frozen. In the second ICSI attempt, 17 oocytes were retrieved: 5 were mature, 1 was immature, and the rest were ZP free or empty follicles. Two of the five MII oocytes were fertilized, one of which was arrested at 4-cell stage and the other developed into a 6-cell embryo and was frozen. The previous three embryos were not successfully implanted after frozen-thawed embryo transfer. Subsequently in the third ICSI attempt, ZP-thin MII oocytes, naked oocytes, and empty follicles were obtained (Figure 1A). Two fertilized oocytes developed into low-quality embryos but failed to implant and the other MII oocytes either did not fertilize or failed to develop into viable embryos after fertilization (Figure 1B).

### Identification of pathogenic variant in *ZP2*

Whole-exome sequencing of proband's peripheral blood was performed to identify possible gene mutations. We identified a novel heterozygous missense variant of c.1616C>T (p.Thr539Met) in *ZP2* in the patient. Sanger sequencing revealed that the mutation was inherited from the father and her sister also carried the same mutation (Figures 2A and 2B). The bases shown in the peak map were reverse complementary sequences of the detected bases. The altered amino acid was located in ZP-C subdomain of ZP2, and this position was highly conserved in most mammalian species (Figure 2C). Using PyMOL software, we performed $ZP2^{WT}$ and $ZP2^{T539M}$ protein structures based on the mouse ZP2 model (PDB ID: 5BUP) (Figure 2D). As predicted, Thr539 was located in a β-sheet and formed hydrogen bonds with Ser541, Tyr603, and His605 to stabilize the protein structure. Thr was polar and hydrophilic, whereas the mutated Met residue was nonpolar and hydrophobic, and Met539 formed hydrogen bonds with only Tyr603. Changes in amino acid characteristics and interactions suggested that $ZP2^{T539M}$ mutation might affect ZP2 structure stability.

### The mutation affected the expression and secretion of ZP2 in 293T cells

To clarify whether the mutation was pathogenic, we constructed $ZP2^{WT}$ and $ZP2^{T539M}$ expression vectors and then transfected them into 293T cells. We transfected $ZP2^{WT}$ plasmid to represent wild type, simultaneously transfected $ZP2^{WT}$ and $ZP2^{T539M}$ plasmids to simulate heterozygous mutation, and transfected $ZP2^{T539M}$ plasmid solely to simulate homozygous mutation. Cell lysates and supernatants were collected 48 h post-transfection for western blotting to detect ZP2 levels. We found that ZP2 was normally expressed in $ZP2^{WT/T539M}$ group compared to $ZP2^{WT}$ group, while ZP2 expression was decreased in $ZP2^{T539M}$ group (Figures 3A and 3B). The ZP2 levels in the supernatant were considerably

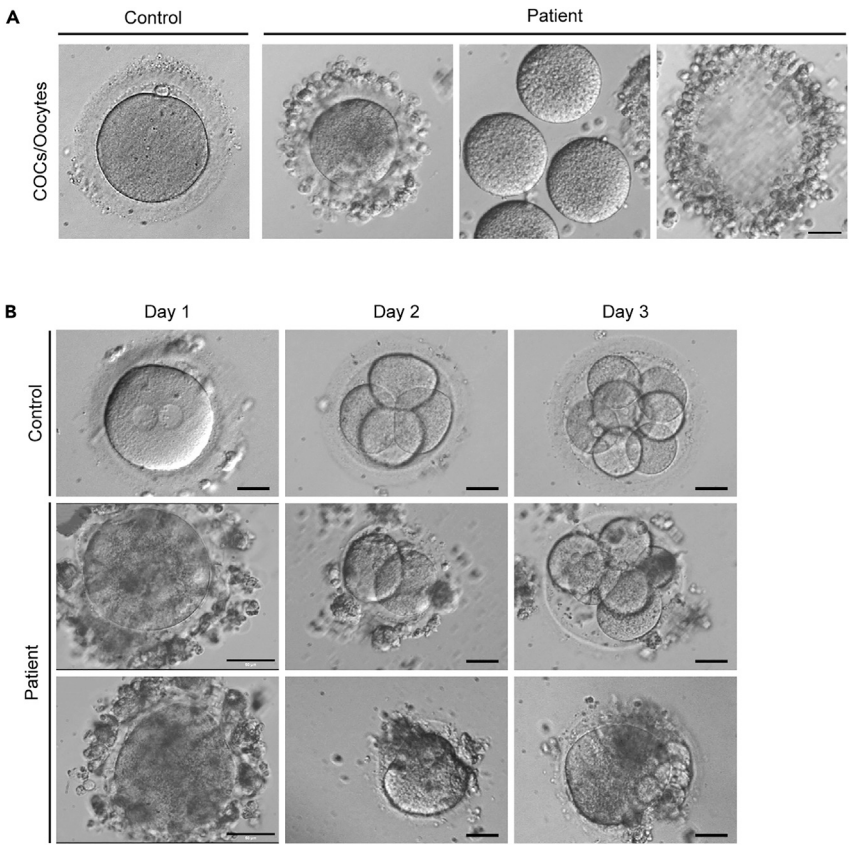


**Figure 1. Clinical characterization**

(A) Images of oocytes or COCs from the control and patient with the *ZP2* heterozygous mutation. Scale bar, 50 μm.

(B) The morphology of early embryogenesis from ICSI-treated MII oocytes from the control and proband. Scale bar, 50 μm.

reduced in $ZP2^{WT/T539M}$ and almost undetectable in $ZP2^{T539M}$ group, showing that intracellular ZP2 failed to be secreted into the media (Figures 3A and 3C). These results suggested that this mutation impaired expression and secretion of ZP2, and this effect was dose dependent with more severe affection in homozygous $ZP2^{T539M}$ group. By immunofluorescent staining, we found that ZP2 was diffusely distributed in the cytoplasm and homozygous mutant ZP2 had significantly weaker signals than wild-type ZP2 (Figures 3D and 3E).

## $Zp2^{T541M}$ female mice were infertile with oocytes lacking the ZP

As evolutionally conserved, the ZP2 sequence was highly consistent in human and mouse.[29] To further explore the impact of the mutation *in vivo*, we generated a mouse model by missense mutation of nucleotides 1622–1623 (CT>TG) on exon14 in mouse *Zp2* using CRISPR-Cas9 technology (Figure 4A). After genotyping and mouse propagation, $Zp2^{WT/T541M}$ heterozygous mutant mice and $Zp2^{T541M}$ homozygous mutant mice were obtained (Figure 4B), and the fertility of $Zp2^{WT/T541M}$ and $Zp2^{T541M}$ male mice was normal.

In order to investigate the effect of $Zp2^{T541M}$ on female fertility, $Zp2^{WT}$, $Zp2^{WT/T541M}$ and $Zp2^{T541M}$ females were mated with fertile males. We found that $Zp2^{T541M}$ female mice were completely infertile, whereas $Zp2^{WT/T541M}$ female mice had normal fertility (Figure 4C). Then, we checked the oocyte number and morphology through superovulation. The numbers of oocytes per mouse were comparable between $Zp2^{WT}$ and $Zp2^{WT/T541M}$ female mice ($Zp2^{WT}$: 19.22 ± 3.96, $Zp2^{WT/T541M}$: 18.40 ± 2.37; $p > 0.05$), while those of $Zp2^{T541M}$ female mice were significantly decreased ($Zp2^{T541M}$: 1.00 ± 0.36, $Zp2^{WT}$: 19.22 ± 3.96; $p < 0.01$) (Figure 4D). Only 1–2 oocytes were obtained from each homozygous mutant female mouse, and most oocytes were degenerated (Figure 4E). Additionally, the ZP thickness of $Zp2^{WT/T541M}$ oocytes was thinner than that of $Zp2^{WT}$ oocytes ($Zp2^{WT}$: 8.26 ± 0.09 μm, $Zp2^{T541M}$: 5.42 ± 0.14 μm; $p < 0.001$), and almost all the $Zp2^{T541M}$ eggs completely lacked ZP (Figures 4E and 4F).

## Aberrant expression, secretion, and localization of mutant ZP2 hindered ZP formation

Since ZP forms gradually with the growth of oocyte, we explored its formation in $Zp2^{T541M}$ oocytes by periodic acid schiff (PAS) staining. In $Zp2^{WT}$ and $Zp2^{WT/T541M}$ ovaries, the ZP was stained magenta and located at periphery of oocytes in follicles at all stages (Figure 5A). Magenta signals were visible in primary and secondary follicles of $Zp2^{T541M}$ ovaries, while disappeared in tertiary follicles (Figure 5A). These results

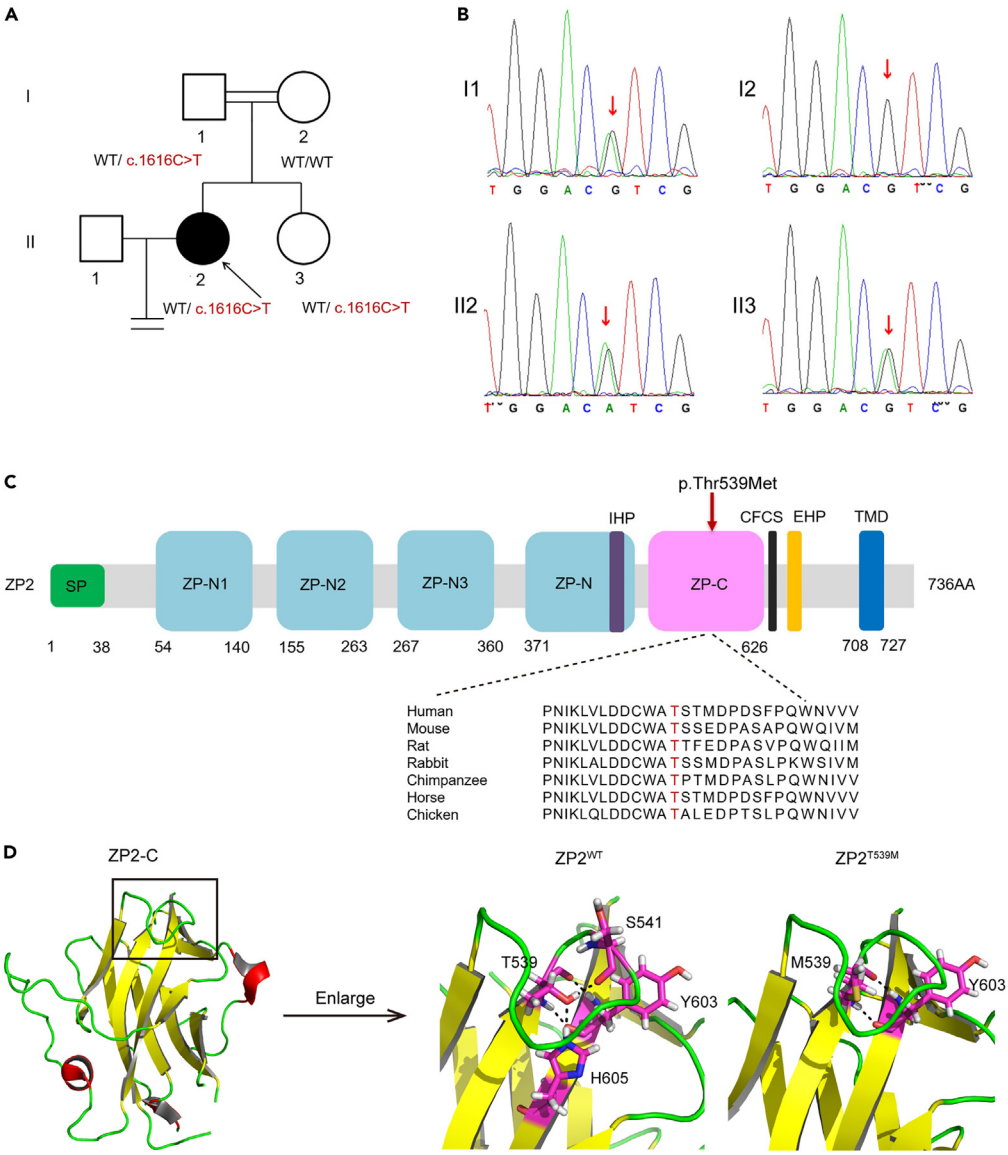


**Figure 2. The heterozygous missense mutation in *ZP2* was identified**

(A) Pedigree of the *ZP2* pathogenic mutation. Square represented male, circle represented female, solid circle represented affected members, equal sign represented infertility, and the arrow indicated the proband, WT represented wild type. (B) Sanger sequencing results of *ZP2* gene from the patient and her family members.

(C) Location and conservation of the mutation in ZP2 protein. ZP2 contains 736 amino acids, including signal peptide (SP), ZP domain (ZPD) consisting of ZP-N and ZP-C subdomains, consensus furin cleavage site (CFCS), internal hydrophobic peptide (IHP), external hydrophobic peptide (EHP), and transmembrane domain (TMD). The red arrow indicated the position of mutated amino acid and the Thr539 was highly conserved in multiple species.

(D) Structure prediction of $ZP2^{WT}$ and $ZP2^{T539M}$ protein by PyMOL software. The overall structure of ZP2-C subdomain was shown on the left, with the black box representing the region of the mutation site. The enlarged structure, on the right, displayed interaction of Thr539/Met539 with surrounding amino acids. Red represented α-helixes, yellow represented β-sheets, and green represented loops. Black dashed line represented hydrogen bonds.

suggested that ZP could be formed in early follicles but not sustained in antral follicles in $Zp2^{T541M}$ female mice. We speculated that ZP deficiency may be caused by the abnormalities in ZP2, so we performed immunofluorescent staining of ZP2 on ovarian sections from 2-month-old mice. Compared to the ring-shaped green signals in $Zp2^{WT}$ and $Zp2^{WT/T541M}$ ovaries, ZP2 was diffusely distributed in the cytoplasm of oocyte and failed to localize in extracellular matrix in $Zp2^{T541M}$ ovary (Figure 5B).

Subsequently, we used the $Zp2^{WT}$ and $Zp2^{T541M}$ plasmid to verify the expression and secretion of ZP2. According to western blotting analysis, $Zp2^{WT/T541M}$ reduced ZP2 contents in the media and $Zp2^{T541M}$ decreased ZP2 levels in the cell lysate and media (Figures 5C–5E). These findings were consistent with the results of human *ZP2* plasmids transfection experiments (Figures 3A–3C), suggesting that the mutation

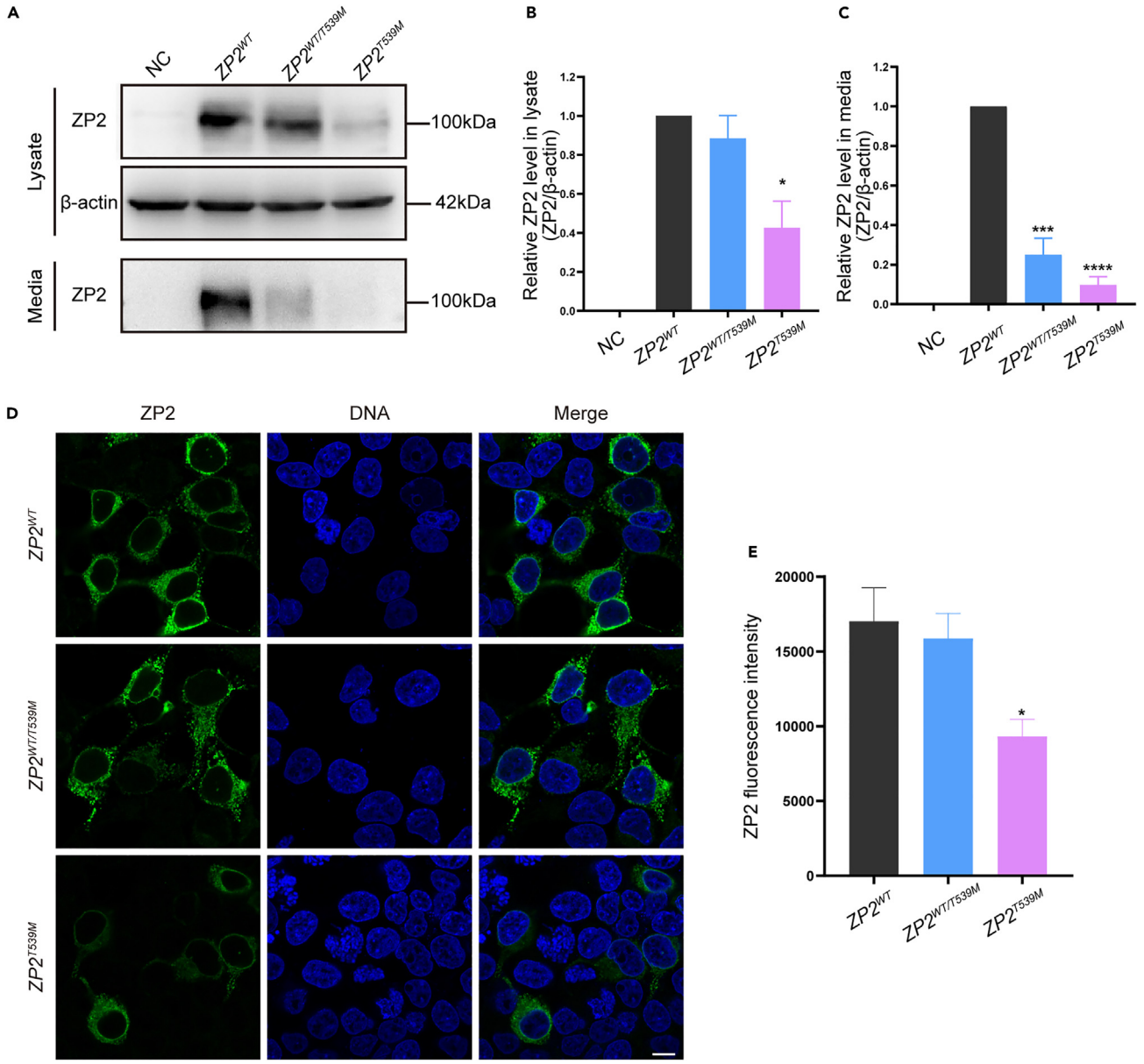


**Figure 3. The missense mutation caused reduced ZP2 expression and secretion**

(A) The ZP2 of cell lysate and media in 293T cells transfected with $ZP2^{WT}$, $ZP2^{WT/T539M}$, and $ZP2^{T539M}$ vectors by western blotting. The molecular weight of ZP2 was 100 kDa, and the molecular weight of β-actin was 42 kDa.

(B) Statistical analysis of relative ZP2 level in cell lysate of each group.

(C) Statistical analysis of relative ZP2 level in media of each group.

(D) Localization of ZP2 in 293T cells transfected with $ZP2^{WT}$, $ZP2^{WT/T539M}$, and $ZP2^{T539M}$ vectors. Green, ZP2; blue, DNA; scale bar, 10 μm.

(E) ZP2 immunofluorescent intensity in three groups. All experiments were repeated at least three times. Data were presented as mean ± SEM, *$p < 0.05$, ***$p < 0.001$, ****$p < 0.0001$.

caused ZP2 intracellular sequestration, prevented ZP2 from being transported to the extracellular matrix and participating in assembly of ZP, and subsequently resulted in aberrant ZP.

## Impaired follicle development in $Zp2^{T541M}$ female mice

Given reduced ovulated eggs of $Zp2^{T541M}$ female mice (Figure 4C), we speculated that follicle development may be impacted by ZP deficiency in $Zp2^{T541M}$ female mice. Therefore, we performed H&E staining and follicle quantification on ovarian sections from

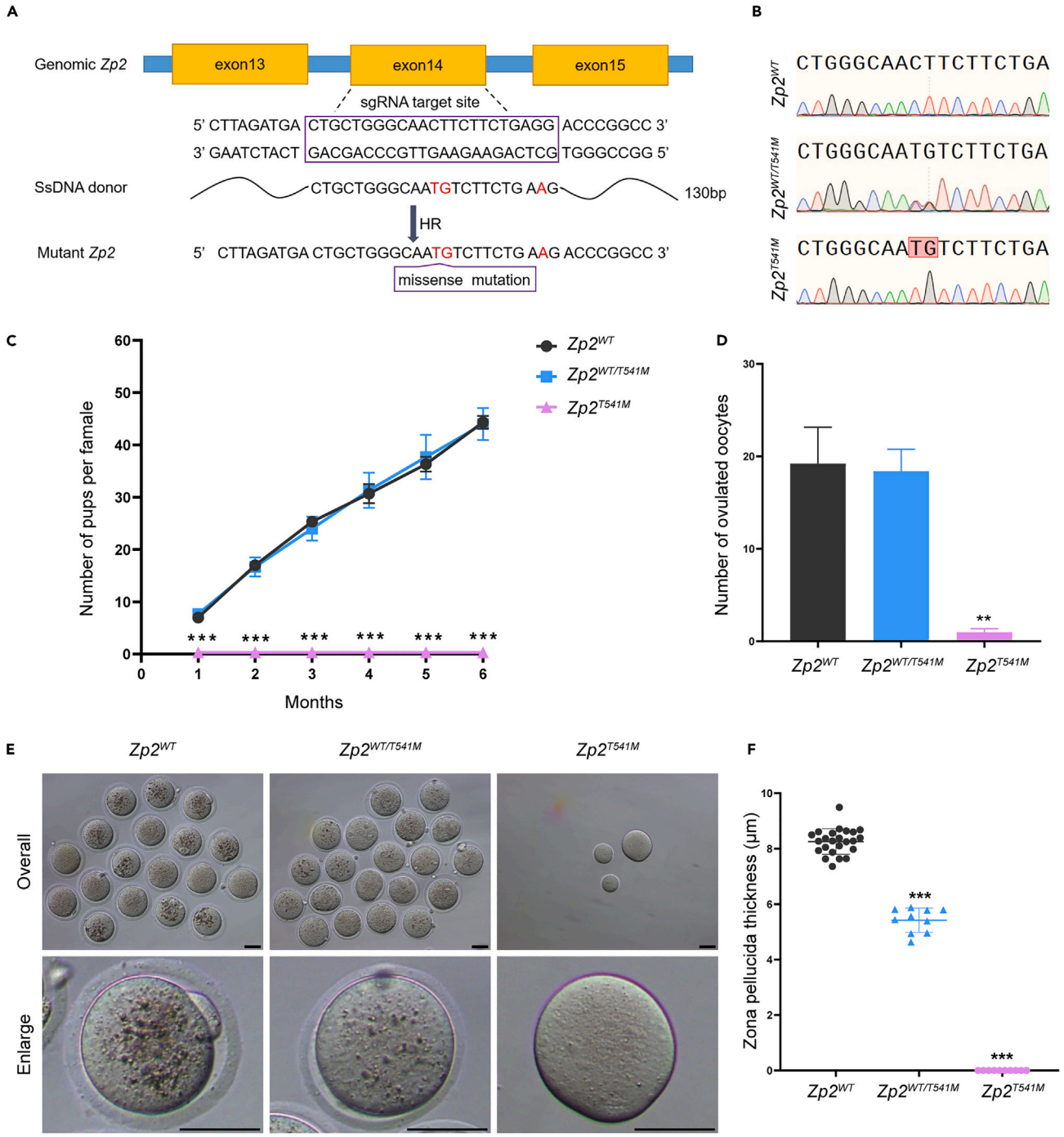


**Figure 4. *Zp2*$^{T541M}$ female mice were infertile**

(A) Schematic diagram of the preparation of *Zp2* mutant mice using CRISPR-Cas9 technology. c.1622-1623CT>TG located in exon14 was the missense mutation. c.1632G>A was a deliberately introduced synonymous mutation. SsDNA: single-stranded DNA; sgRNA: single-guide RNA; HR: homologous recombination.

(B) Gene sequences of *Zp2*$^{WT}$, *Zp2*$^{WT/T541M}$, and *Zp2*$^{T541M}$ mice were identified by Sanger sequencing. The bases in the red box were the mutant.

(C) Fertility curves showed the total number of litters per female for 6 months. At least 3 female mice of each genotype were used in the experiment.

(D) The numbers of MII oocytes in female mice of three groups after superovulation treatment.

(E)The bright-field images from superovulated *Zp2*$^{WT}$, *Zp2*$^{WT/T541M}$ and *Zp2*$^{T541M}$ MII oocytes of 6-week-old mice. Bar, 100 μm.

(F) ZP thickness of MII oocytes for each group. All experiments were repeated at least three times. Data were presented as mean ± SEM, *p < 0.05, **p < 0.01, ***p < 0.001.

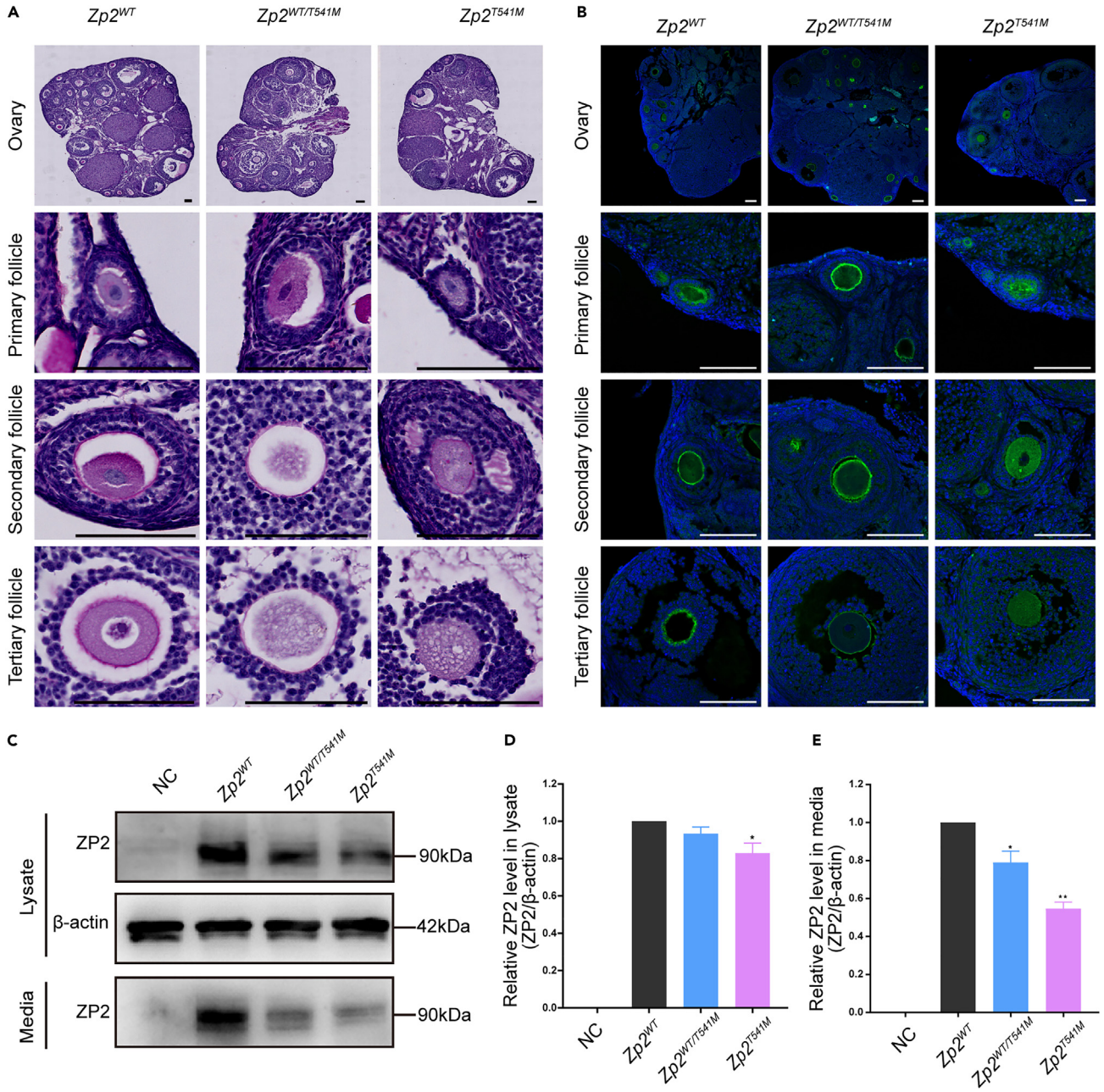


**Figure 5. *Zp2*$^{T541M}$ mutation interfered with ZP2 secretion and ZP formation**

(A) PAS staining images of ovarian sections in 2-month-old *Zp2*$^{WT}$, *Zp2*$^{WT/T541M}$, and *Zp2*$^{T541M}$ female mice. Bar, 100 μm.

(B) Immunofluorescent staining of ZP2 in 2-month-old *Zp2*$^{WT}$, *Zp2*$^{WT/T541M}$, and *Zp2*$^{T541M}$ ovarian sections. Green, ZP2; blue, DNA; bar, 100 μm.

(C) Western blot analysis of ZP2 in cell lysate and media of 3T3 cells transfected with *Zp2*$^{WT}$, *Zp2*$^{WT/T541M}$, and *Zp2*$^{T541M}$ vectors. The molecular weight of ZP2 was 90 kDa, and the molecular weight of β-actin was 42 kDa.

(D) Statistical analysis of relative ZP2 expression level in cell lysate of each group.

(E) Statistical analysis of relative ZP2 secretion level in media of each group. All experiments were repeated at least three times. Data were presented as mean ± SEM,*$p < 0.05$, **$p < 0.01$.

2-month-old *Zp2*$^{WT}$, *Zp2*$^{WT/T541M}$, and *Zp2*$^{T541M}$ female mice (Figure 6A). There was no significant difference in the numbers of follicles at all stages between *Zp2*$^{WT}$ and *Zp2*$^{WT/T541M}$ mice, but a marked reduction in tertiary follicles of *Zp2*$^{T541M}$ homozygous mutant mice was observed (Figure 6B).

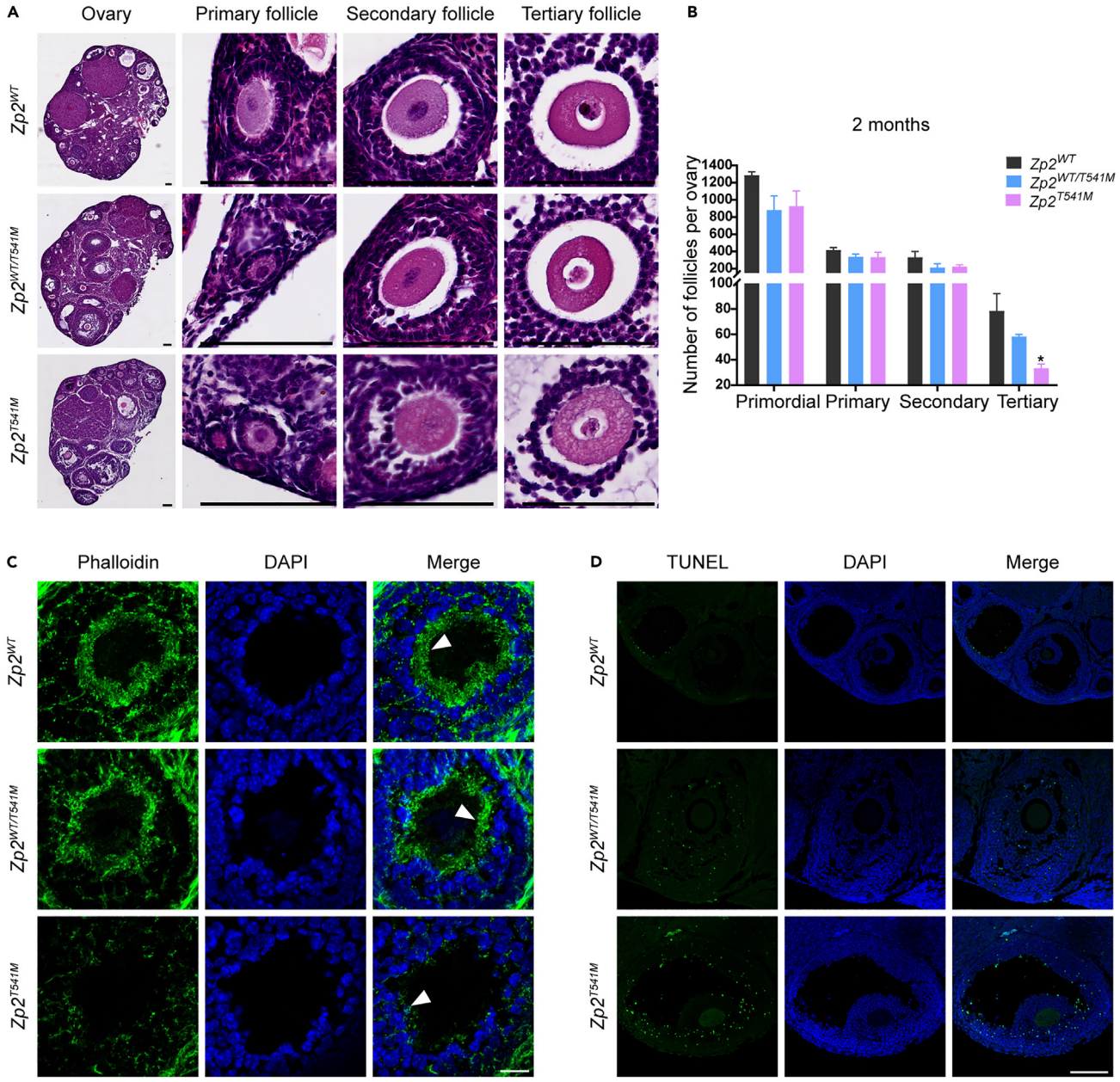


**Figure 6. Defected folliculogenesis in $Zp2^{T541M}$ female mice**

(A) H&E staining of ovarian sections in 2-month-old $Zp2^{WT}$, $Zp2^{WT/T541M}$, and $Zp2^{T541M}$ female mice. Bar, 100 μm.

(B) Quantification of follicles at all stages in ovaries from three groups. At least three female mice of each genotype were used. Data were presented as mean ± SEM, *p < 0.05.

(C) Phalloidin staining of frozen ovarian sections from 2-month-old female mice. Green, Phalloidin; blue, DAPI; white arrowheads, TZPs; bar, 20 μm.

(D) Ovarian paraffin sections from 2-month-old female mice were stained with TUNEL. Green, TUNEL; blue, DAPI; bar, 100 μm.

Phalloidin and TUNEL immunofluorescent staining were performed on 2-month-old ovarian sections to explore the reason for impaired follicle development in $Zp2^{T541M}$ female mice. We found that the tertiary follicles contained abundant and dense signs of transzonal projections (TZPs) in $Zp2^{WT}$ and $Zp2^{WT/T541M}$ ovaries, whereas the signs were sparse or even absent in $Zp2^{T541M}$ tertiary follicles (Figure 6C). More apoptotic granulosa cells were found in antral follicles from $Zp2^{T541M}$ female ovary (Figure 6D). These results suggested that reduced number of tertiary follicles in $Zp2^{T541M}$ female mice may be due to the fact that decreased numbers of TZPs disrupted the communications between oocyte and granulosa cells, which in turn caused increase in apoptotic granulosa cells and further resulted in atretic follicles.

## DISCUSSION

In female reproduction, the production of a fertilizable egg is dependent on the collaboration of follicle development and oocyte growth. As the coat of oocyte, ZP is crucial to oogenesis, fertilization, and early embryo development. Therefore, ZP is often used as an indicator of oocyte quality in assisted reproduction treatment. ZP aberrations account for 2%–5% of all oocytes.[30,31] Statistically, ZP dysmorphology resulted in a 30% reduction in clinical pregnancy rates.[32] Previous studies showed that various variants in *ZP1*, *ZP2*, *ZP3*, and *ZP4* may cause ZP abnormalities, female infertility, and assisted reproductive treatment failure.[25,33] In general, mutations near the N terminus had severe effects, and patients ovulated degenerated oocytes or even showed empty follicle syndrome (EFS).[23,34,35] Mutations occurring in CFCS or TMD often affected secretion of zona pellucida proteins, resulting in thin ZP.[36,37] When missense or frameshift mutation sites were located in ZPD, the expressed proteins might interact abnormally with other zona pellucida proteins, affecting the assembly and polymerization of ZP, leading to oocyte degeneration, thin ZP or absence of ZP, and even EFS.[27,38–40]

In this study, we identified the heritable heterozygous mutation (c.1616C>T, p.Thr539Met) in *ZP2* from an infertile family. The oocytes retrieved from the patient lacked ZP, had ZP without oocyte cytoplasm, or looked normal but failed to implant after fertilization. The mutation was located in ZP-C subdomain, which was an antiparallel β-sheet sandwich composed of eight strands of polypeptide chains.[41] Bioinformatic analysis showed that the mutation located at the end of one polypeptide chain might affect formation of β-sheet and the stability of ZP2 protein.

We found that the mutation impaired the expression and secretion of ZP2 using transfected 293T cells. Next, the mutant mouse model was introduced. Interestingly, $Zp2^{WT/T541M}$ female mice were fertile with ZP-thin eggs, which was inconsistent with the phenotype of infertile female caused by *ZP2* heterozygous mutation. Similarly, a previous report mentioned that homozygous 8-bp deletion mutation of *ZP1* (c.1169_1176delTTTTCCCA) in humans was fully infertile, while the corresponding mutant mice were fertile.[42] The different phenotypes of the same gene mutation of zona pellucida in human and mouse may be due to the difference in the numbers and assembly mechanism of zona pellucida protein.[42] In mice, ZP2-ZP3 heterodimers formed 14-nm repetitive structure elements to produce μm-long ZP filaments, which were cross-linked by ZP1 homodimers to form a mesh-like matrix.[41,43] Human ZP comprised of filaments formed by heterodimers of ZP3 and either ZP2 or ZP4. ZP1 occasionally replaced ZP2/ZP4 for embedding in fibers and cross-linked between filaments.[41,44] These differences might lead to human oocytes being more sensitive to ZP defects and having poorer development potential.

In order to determine the reason why $Zp2^{T541M}$ female mice were sterile, COCs were obtained from the fallopian tubes under the administration of appropriate gonadotropins stimulation. After digestion by hyaluronidase, COCs of $Zp2^{T541M}$ female mice were mostly empty mucus masses with few mature eggs, and a small proportion contained degenerate oocytes, similar to EFS due to zona pellucida gene mutations. We found that the ZP was absent in $Zp2^{T541M}$ tertiary follicles and the mutant ZP2 was abnormally localized in the cytoplasm. Meanwhile, the results of *in vitro* transfection experiments also confirmed that $Zp2^{T541M}$ mutation blocked ZP2 secretion. These results suggested that mutant forms of ZP2 were retained within cells and failed to be transported extracellularly to participate in zona pellucida protein-protein polymerization, resulting in ZP loss in $Zp2^{T541M}$ female mice and a thin ZP due to expression and secretion of a portion of wild-type ZP2 protein in $Zp2^{WT/T541M}$ female mice. Interestingly, the ZP was still present in primary and secondary follicles in the ovaries of $Zp2^{T541M}$ female mice. Similarly, a previous study by Rankin and colleagues showed that ZP was eliminated in the preovulatory follicles but present in early follicles as a thin ZP synthesized by ZP1 and ZP3 in *Zp2* knockout mice.[17] These findings suggested that ZP2 may not be necessary for ZP during early follicular development, but may be indispensable for the formation of a structurally stable ZP during late follicular development.

TZPs are microvillous structures formed by the extension of cytoplasmic filaments from granulosa cells across ZP to the plasma membrane of oocytes.[45] TZPs provided a structural basis for bidirectional communications between oocyte and surrounding granulosa cells.[46,47] The number of TZPs was reduced in *Gdf9*-deficient mice, and they were often parallel rather than perpendicular to the oocyte surface, indicating that the oocyte might also be involved in the formation of TZPs.[48] In 2021, oocyte-derived microvilli were identified by high-resolution live-cell imaging system, which promoted TZPs construction by regulating release of oocyte-secreted factors.[49] We found that $Zp2^{T541M}$ tertiary follicles contained dramatically lower TZPs. Also, there were significantly increased apoptotic signals in granulosa cells of $Zp2^{T541M}$ tertiary follicles. These findings indicated that $Zp2^{T541M}$ mutation in female mice caused ZP deletion which blocked oocyte-granulosa cell communications and impaired folliculogenesis, resulting in an obvious decrease in the number of antral follicles and ovulated eggs, and subsequently complete female infertility.

In conclusion, the novel variant (c. C1616 > T, p.Thr539Met) at ZP-C subdomain in *ZP2* was identified to be related to female infertility. The mutation was deleterious for expression and secretion of ZP2 protein, formation of ZP, follicle development, and oocyte quality, as verified by the cell lines and mouse model. The study not only finds a novel pathogenic *ZP2* point mutation causing female infertility but also more importantly provides new mechanistic insights into how ZP gene mutations cause female fertility.

### Limitations of the study

Due to the rarity of human samples, we had identified the *ZP2* mutation (c. C1616 > T, p.Thr539Met) from one family. Besides, further investigation is needed to explore the molecular mechanisms underlying the difference between healthy $Zp2^{WT/T541M}$ oocytes and degenerated $Zp2^{T541M}$ oocytes.

## STAR★METHODS

Detailed methods are provided in the online version of this paper and include the following:

- KEY RESOURCES TABLE
- RESOURCE AVAILABILITY

## ACKNOWLEDGMENTS

We thank the proband and her family for their support and participation. We are grateful for technical assistance from Shi-Wen Li, Xi-Li Zhu, and Hua Qin. This study was supported by the National R&D Program of China (2022YFA0806302), the National Natural Science Foundation of China (82171646), and Strategic Collaborative Research Program of the Ferring Institute of Reproductive Medicine (FIRMC200507).

## AUTHOR CONTRIBUTIONS

Z.W. designed the research. Z.W. and Q.S. guided and supervised the experiments. S.L., B.Z., and J.G. performed the experiments and analyzed the data. H.Z. and W.W. provided clinical patient information. W.-B.L., W.-L.L., Y.L., Z.H., Y.O., and Y.H. provided advice and assistance for the experiments. S.L. and Z.W. wrote the manuscript. All authors read and approved the manuscript.

## DECLARATION OF INTERESTS

The authors declare no competing interests.

Received: May 16, 2023
Revised: July 24, 2023
Accepted: September 1, 2023
Published: September 4, 2023

## REFERENCES

1. Litscher, E.S., and Wassarman, P.M. (2020). Zona Pellucida Proteins, Fibrils, and Matrix. Annu. Rev. Biochem. *89*, 695–715. https://doi.org/10.1146/annurev-biochem-011520-105310.
2. Gilchrist, R.B., Lane, M., and Thompson, J.G. (2008). Oocyte-secreted factors: regulators of cumulus cell function and oocyte quality. Hum. Reprod. Update *14*, 159–177. https://doi.org/10.1093/humupd/dmm040.
3. Matzuk, M.M., Burns, K.H., Viveiros, M.M., and Eppig, J.J. (2002). Intercellular communication in the mammalian ovary: oocytes carry the conversation. Science (New York, N.Y.) *296*, 2178–2180. https://doi.org/10.1126/science.1071965.
4. Pang, P.C., Chiu, P.C.N., Lee, C.L., Chang, L.Y., Panico, M., Morris, H.R., Haslam, S.M., Khoo, K.H., Clark, G.F., Yeung, W.S.B., and Dell, A. (2011). Human Sperm Binding Is Mediated by the Sialyl-Lewis(x) Oligosaccharide on the Zona Pellucida. Science (New York, N.Y.) *333*, 1761–1764. https://doi.org/10.1126/science.1207438.
5. Tokuhiro, K., and Dean, J. (2018). Glycan-Independent Gamete Recognition Triggers Egg Zinc Sparks and ZP2 Cleavage to Prevent Polyspermy. Dev. Cell *46*, 627–640.e5. https://doi.org/10.1016/j.devcel.2018.07.020.
6. Burkart, A.D., Xiong, B., Baibakov, B., Jiménez-Movilla, M., and Dean, J. (2012). Ovastacin, a cortical granule protease, cleaves ZP2 in the zona pellucida to prevent polyspermy. J. Cell Biol. *197*, 37–44. https://doi.org/10.1083/jcb.201112094.
7. Familiari, G., Heyn, R., Relucenti, M., and Sathananthan, H. (2008). Structural changes of the zona pellucida during fertilization and embryo development. Front. Biosci. *13*, 6730–6751. https://doi.org/10.2741/3185.
8. Michelmann, H.W., Rath, D., Töpfer-Petersen, E., and Schwartz, P. (2007). Structural and functional events on the porcine zona pellucida during maturation, fertilization and embryonic development: a scanning electron microscopy analysis. Reprod. Domest. Anim. *42*, 594–602. https://doi.org/10.1111/j.1439-0531.2006.00829.x.
9. Gupta, S.K. (2021). Human Zona Pellucida Glycoproteins: Binding Characteristics With Human Spermatozoa and Induction of Acrosome Reaction. Front. Cell Dev. Biol. *9*, 619868. https://doi.org/10.3389/fcell.2021.619868.
10. Izquierdo-Rico, M.J., Moros-Nicolás, C., Pérez-Crespo, M., Laguna-Barraza, R., Gutiérrez-Adán, A., Veyrunes, F., Ballesta, J., Laudet, V., Chevret, P., and Avilés, M. (2020). ZP4 Is Present in Murine Zona Pellucida and Is Not Responsible for the Specific Gamete Interaction. Front. Cell Dev. Biol. *8*, 626679. https://doi.org/10.3389/fcell.2020.626679.
11. Gupta, S.K. (2018). The Human Egg's Zona Pellucida. Curr. Top. Dev. Biol. *130*, 379–411. https://doi.org/10.1016/bs.ctdb.2018.01.001.
12. Jovine, L., Qi, H., Williams, Z., Litscher, E., and Wassarman, P.M. (2002). The ZP domain is a conserved module for polymerization of extracellular proteins. Nat. Cell Biol. *4*, 457–461. https://doi.org/10.1038/ncb802.
13. Bork, P., and Sander, C. (1992). A large domain common to sperm receptors (Zp2 and Zp3) and TGF-beta type III receptor.

FEBS Lett. *300*, 237–240. https://doi.org/10.1016/0014-5793(92)80853-9.

14. Jovine, L., Qi, H., Williams, Z., Litscher, E.S., and Wassarman, P.M. (2004). A duplicated motif controls assembly of zona pellucida domain proteins. Proc. Natl. Acad. Sci. USA *101*, 5922–5927. https://doi.org/10.1073/pnas.0401600101.
15. Jimenez-Movilla, M., and Dean, J. (2011). ZP2 and ZP3 cytoplasmic tails prevent premature interactions and ensure incorporation into the zona pellucida. J. Cell Sci. *124*, 940–950. https://doi.org/10.1242/jcs.079988.
16. Wassarman, P.M., and Litscher, E.S. (2018). The Mouse Egg's Zona Pellucida. Curr. Top. Dev. Biol. *130*, 331–356. https://doi.org/10.1016/bs.ctdb.2018.01.003.
17. Rankin, T.L., O'Brien, M., Lee, E., Wigglesworth, K., Eppig, J., and Dean, J. (2001). Defective zonae pellucidae in Zp2-null mice disrupt folliculogenesis, fertility and development. Development *128*, 1119–1126. https://doi.org/10.1242/dev.128.7.1119.
18. Liu, C., Litscher, E.S., Mortillo, S., Sakai, Y., Kinloch, R.A., Stewart, C.L., and Wassarman, P.M. (1996). Targeted disruption of the mZP3 gene results in production of eggs lacking a zona pellucida and infertility in female mice. Proc. Natl. Acad. Sci. USA *93*, 5431–5436. https://doi.org/10.1073/pnas.93.11.5431.
19. Rankin, T., Talbot, P., Lee, E., and Dean, J. (1999). Abnormal zonae pellucidae in mice lacking ZP1 result in early embryonic loss. Development *126*, 3847–3855. https://doi.org/10.1242/dev.126.17.3847.
20. Huang, H.L., Lv, C., Zhao, Y.C., Li, W., He, X.M., Li, P., Sha, A.G., Tian, X., Papasian, C.J., Deng, H.W., et al. (2014). Mutant ZP1 in familial infertility. N. Engl. J. Med. *370*, 1220–1226. https://doi.org/10.1056/NEJMoa1308851.
21. Lv, C., Huang, H.L., Yi, D.J., Peng, T.L., Tan, H.J., Quan, R.P., Deng, H.W., and Xiao, H.M. (2021). Mutant Zp1 impedes incorporation of ZP3 and ZP4 in the zona pellucida, resulting in zona absence and female infertility in ratsdagger. Biol. Reprod. *104*, 1262–1270. https://doi.org/10.1093/biolre/ioab025.
22. Wei, X., Li, Y., Liu, Q., Liu, W., Yan, X., Zhu, X., Zhou, D., Tian, Y., Zhang, F., Li, N., and Lu, Z. (2022). Mutations in ZP4 are associated with abnormal zona pellucida and female infertility. J. Clin. Pathol. *75*, 201–204. https://doi.org/10.1136/jclinpath-2020-207170.
23. Zhou, Z., Ni, C., Wu, L., Chen, B., Xu, Y., Zhang, Z., Mu, J., Li, B., Yan, Z., Fu, J., et al. (2019). Novel mutations in ZP1, ZP2, and ZP3 cause female infertility due to abnormal zona pellucida formation. Hum. Genet. *138*, 327–337. https://doi.org/10.1007/s00439-019-01990-1.
24. Zhou, J., Wang, M., Yang, Q., Li, D., Li, Z., Hu, J., Jin, L., and Zhu, L. (2022). Can successful pregnancy be achieved and predicted from patients with identified ZP mutations? A literature review. Reprod. Biol. Endocrinol. *20*, 166. https://doi.org/10.1186/s12958-022-01046-6.
25. Litscher, E.S., and Wassarman, P.M. (2020). Zona pellucida genes and proteins and human fertility. Trends Dev. Biol. *13*, 21–33.
26. Dai, C., Hu, L., Gong, F., Tan, Y., Cai, S., Zhang, S., Dai, J., Lu, C., Chen, J., Chen, Y., et al. (2019). ZP2 pathogenic variants cause *in vitro* fertilization failure and female infertility. Genet. Med. *21*, 431–440. https://doi.org/10.1038/s41436-018-0064-y.
27. Yang, P., Luan, X., Peng, Y., Chen, T., Su, S., Zhang, C., Wang, Z., Cheng, L., Zhang, X., Wang, Y., et al. (2017). Novel zona pellucida gene variants identified in patients with oocyte anomalies. Fertil. Steril. *107*, 1364–1369. https://doi.org/10.1016/j.fertnstert.2017.03.029.
28. Sun, Y., Zeng, Y., Chen, H., Zhou, Z., Fu, J., Sang, Q., Wang, L., Sun, X., Chen, B., and Xu, C. (2021). A novel homozygous variant in ZP2 causes abnormal zona pellucida formation and female infertility. J. Assist. Reprod. Genet. *38*, 1239–1245. https://doi.org/10.1007/s10815-021-02107-2.
29. Litscher, E.S., and Wassarman, P.M. (2014). Evolution, structure, and synthesis of vertebrate egg-coat proteins. Trends Dev. Biol. *8*, 65–76.
30. Rienzi, L., Vajta, G., and Ubaldi, F. (2011). Predictive value of oocyte morphology in human IVF: a systematic review of the literature. Hum. Reprod. Update *17*, 34–45. https://doi.org/10.1093/humupd/dmq029.
31. Balaban, B., Urman, B., Sertac, A., Alatas, C., Aksoy, S., and Mercan, R. (1998). Oocyte morphology does not affect fertilization rate, embryo quality and implantation rate after intracytoplasmic sperm injection. Hum. Reprod. *13*, 3431–3433. https://doi.org/10.1093/humrep/13.12.3431.
32. Sauerbrun-Cutler, M.T., Vega, M., Breborowicz, A., Gonzales, E., Stein, D., Lederman, M., and Keltz, M. (2015). Oocyte zona pellucida dysmorphology is associated with diminished in-vitro fertilization success. J. Ovarian Res. *8*, 5. https://doi.org/10.1186/s13048-014-0111-5.
33. Wassarman, P.M., and Litscher, E.S. (2022). Female fertility and the zona pellucida. Elife *11*, e76106. https://doi.org/10.7554/eLife.76106.
34. Xu, Q., Zhu, X., Maqsood, M., Li, W., Tong, X., Kong, S., Wang, F., Liu, X., Wei, Z., Zhang, Z., et al. (2020). A novel homozygous nonsense ZP1 variant causes human female infertility associated with empty follicle syndrome (EFS). Mol. Genet. Genomic Med. *8*, e1269. https://doi.org/10.1002/mgg3.1269.
35. Wu, L., Li, M., Yin, M., Ou, Y., Yan, Z., Kuang, Y., Yan, Z., and Li, B. (2021). Novel mutations in ZP1: Expanding the mutational spectrum associated with empty follicle syndrome in infertile women. Clin. Genet. *99*, 583–587. https://doi.org/10.1111/cge.13921.
36. Liu, W., Li, K., Bai, D., Yin, J., Tang, Y., Chi, F., Zhang, L., Wang, Y., Pan, J., Liang, S., et al. (2017). Dosage effects of ZP2 and ZP3 heterozygous mutations cause human infertility. Hum. Genet. *136*, 975–985. https://doi.org/10.1007/s00439-017-1822-7.
37. Shen, Y., Guo, J., Zhang, X., Wang, X., Zhu, S., Chen, D., Xiong, W., Lu, G., Liu, X., Dai, C., et al. (2022). Identification of a heterozygous variant of ZP2 as a novel cause of empty follicle syndrome in humans and mice. Hum. Reprod. *37*, 859–872. https://doi.org/10.1093/humrep/deac026.
38. Chen, Y., Wang, Z., Wu, Y., He, W., Du, J., Cai, S., Gong, F., Lu, G., Lin, G., and Dai, C. (2021). Case Report: A Novel Heterozygous ZP3 Deletion Associated With Empty Follicle Syndrome and Abnormal Follicular Development. Front. Genet. *12*, 690070. https://doi.org/10.3389/fgene.2021.690070.
39. Dai, C., Chen, Y., Hu, L., Du, J., Gong, F., Dai, J., Zhang, S., Wang, M., Chen, J., Guo, J., et al. (2019). ZP1 mutations are associated with empty follicle syndrome: evidence for the existence of an intact oocyte and a zona pellucida in follicles up to the early antral stage. A case report. Hum. Reprod. *34*, 2201–2207. https://doi.org/10.1093/humrep/dez174.
40. Zhang, D., Zhu, L., Liu, Z., Ren, X., Yang, X., Li, D., Luo, Y., Peng, X., Zhou, X., Jia, W., et al. (2021). A novel mutation in ZP3 causes empty follicle syndrome and abnormal zona pellucida formation. J. Assist. Reprod. Genet. *38*, 251–259. https://doi.org/10.1007/s10815-020-01995-0.
41. Bokhove, M., and Jovine, L. (2018). Structure of Zona Pellucida Module Proteins. Curr. Top. Dev. Biol. *130*, 413–442. https://doi.org/10.1016/bs.ctdb.2018.02.007.
42. Wang, Y., Lv, C., Huang, H.L., Zeng, M.H., Yi, D.J., Tan, H.J., Peng, T.L., Yu, W.X., Deng, H.W., and Xiao, H.M. (2019). Influence of mouse defective zona pellucida in folliculogenesis on apoptosis of granulosa cells and developmental competence of oocytes. Biol. Reprod. *101*, 457–465. https://doi.org/10.1093/biolre/ioz093.
43. Familiari, G., Relucenti, M., Heyn, R., Micara, G., and Correr, S. (2006). Three-dimensional structure of the zona pellucida at ovulation. Microsc. Res. Tech. *69*, 415–426. https://doi.org/10.1002/jemt.20301.
44. Kiefer, S.M., and Saling, P. (2002). Proteolytic processing of human zona pellucida proteins. Biol. Reprod. *66*, 407–414. https://doi.org/10.1095/biolreprod66.2.407.
45. Clarke, H.J. (2018). Regulation of germ cell development by intercellular signaling in the mammalian ovarian follicle. Wiley Interdiscip. Rev. Dev. Biol. *7*. https://doi.org/10.1002/wdev.294.
46. Li, R., and Albertini, D.F. (2013). The road to maturation: somatic cell interaction and self-organization of the mammalian oocyte. Nat. Rev. Mol. Cell Biol. *14*, 141–152. https://doi.org/10.1038/nrm3531.
47. Albertini, D.F., Combelles, C.M., Benecchi, E., and Carabatsos, M.J. (2001). Cellular basis for paracrine regulation of ovarian follicle development. Reproduction *121*, 647–653. https://doi.org/10.1530/rep.0.1210647.
48. Carabatsos, M.J., Elvin, J., Matzuk, M.M., and Albertini, D.F. (1998). Characterization of oocyte and follicle development in growth differentiation factor-9-deficient mice. Dev. Biol. *204*, 373–384. https://doi.org/10.1006/dbio.1998.9087.
49. Zhang, Y., Wang, Y., Feng, X., Zhang, S., Xu, X., Li, L., Niu, S., Bo, Y., Wang, C., Li, Z., et al. (2021). Oocyte-derived microvilli control female fertility by optimizing ovarian follicle selection in mice. Nat. Commun. *12*, 2523. https://doi.org/10.1038/s41467-021-22829-2.
50. Pedersen, T., and Peters, H. (1968). Proposal for a classification of oocytes and follicles in the mouse ovary. J. Reprod. Fertil. *17*, 555–557. https://doi.org/10.1530/jrf.0.0170555.

## STAR★METHODS

### KEY RESOURCES TABLE

| REAGENT or RESOURCE | SOURCE | IDENTIFIER |
|---|---|---|
| Antibodies | | |
| Anti-ZP2 antibody | Boster | Cat#PB0958; |
| Mouse Anti-β actin mAb | Zsgb-bio | Cat#TA-09; RRID: AB_2636897 |
| Myc-tag Monoclonal antibody | ChromoTek | Cat#9E1; RRID: AB_2631398 |
| Alexa Fluor™ 488 phalloidin | Thermo Fisher Scientific | Cat#A12379 |
| HRP conjugated goat anti-Rat IgG | Zsgb-bio | Cat#ZB-2307 |
| HRP goat anti-mouse IgG | Zsgb-bio | Cat#ZB-2305; RRID: AB_2747415 |
| HRP goat anti-rabbit IgG | Zsgb-bio | Cat#ZB-2301; RRID: AB_2747412 |
| Goat anti-rabbit 488 | Invitrogen | Cat#A11034; RRID: AB_2576217 |
| Chemicals, peptides, and recombinant proteins | | |
| M2 medium | Sigma Aldrich | Cat#M7167 |
| DMEM medium | Gibco | Cat#C11965500BT |
| FBS | PAN-Biotech | Cat#ST30-3302 |
| Penicillin and streptomycin | Beyotime | Cat#C0222 |
| 0.25% Trypsin-EDTA | Gibco | Cat#25200-056 |
| Lipofectamine 3000 | Invitrogen | Cat#2328417 |
| RIPA lysis buffer | Beyotime | Cat#P0013B |
| PIC | Roche | Cat#04693159001 |
| Critical commercial assays | | |
| PAS stain kit | Solarbio | Cat#G1280 |
| KOD-Plus-Mutagenesis Kit | Toyobo | Cat #SMK-101 |
| BCA protein assay kit | Biosharp | Cat #BL521A |
| DeadEnd™ Fluorometric TUNEL System | Promega | Cat #G3250 |
| Experimental models: Cell lines | | |
| 293T | Provided by Dr. Lei Li at Institute of Zoology, Chinese Academy of Sciences | N/A |
| NIH-3T3 | Provided by Dr. Lei Li at Institute of Zoology, Chinese Academy of Sciences | N/A |
| Experimental models: Organisms/strains | | |
| C57/BL6 mice | This paper | N/A |
| Oligonucleotides | | |
| Genotyping of Zp2 point mutant mice, forward primer 5′-CCTAATGGATGTTGCAGCCAGC-3′ | This paper | N/A |
| Genotyping of Zp2 point mutant mice, Reverse primer 5′-GCCGTTTGGAGAGAAGCCCAT-3′ | This paper | N/A |
| Recombinant DNA | | |
| PCS2+hZP2 | This paper | N/A |
| pcDNA3.1+mZP2 | This paper | N/A |

(*Continued on next page*)

*Continued*

| REAGENT or RESOURCE | SOURCE | IDENTIFIER |
|---|---|---|
| Software and algorithms | | |
| ImageJ | Wayne Rasband, NIH | https://imagej.nih.gov/ij/ |
| Photoshop CC 2020 | Adobe | N/A |
| Illustrator CC 2019 | Adobe | N/A |
| Prism v8.0.2 | Graphpad | N/A |
| PyMOL 1.8.x | Schrodinger | https://pymol.org/2/ |
| Other | | |
| Amicon Ultra-4 centrifugal filter devices | Millipore | Cat#UFC803096 |
| Whole-exome sequencing data for the infertility female | This paper | https://doi.org/10.57760/sciencedb.10344 |

## RESOURCE AVAILABILITY

### Lead contact

Further information and requests for resources and reagents should be directed to and will be fulfilled by the lead contact, Zhen-Bo Wang (wangzb@ioz.ac.cn).

### Materials availability

This study did not generate new unique reagents.

### Data and code availability

- Whole-exome sequencing data have been deposited at Science Data Bank and are publicly available as of the date of publication. Accession numbers are listed in the key resources table.
- This paper does not report original code.
- Any additional information required to reanalyze the data reported in this paper is available from the lead contact upon request.

## EXPERIMENTAL MODEL AND STUDY PARTICIPANT DETAILS

### Human participants

The patient and healthy control were recruited from the Sixth Medical Center for PLA General Hospital. They were Han Chinese women of childbearing age between 25-45 years old. The study was approved by the ethics committee from the same center. Informed consent for this study was obtained from all participants.

### Mice

$Zp2^{T541M}$ and $Zp2^{WT/T541M}$ mice were provided by the Experimental Animal Center of the Institute of Animal Science, Chinese Academy of Sciences. $Zp2^{WT/T541M}$ mice were crossed to obtain $Zp2^{T541M}$ and $Zp2^{WT/T541M}$ mice. We chose well-grown $Zp2^{T541M}$ and $Zp2^{WT/T541M}$ females at 6–8 weeks old as experimental mice and corresponding $Zp2^{WT}$ female mice as control. Mice are raised in the SPF environment with adequate food, water, and light from 7:00-19:00.

All experimental operations and animal care strictly complied with the guidelines and procedures of the Experimental Animal Ethics Committee of the Institute of Zoology, University of Chinese Academy of Sciences.

### Cell lines and cell culture

293T cells and 3T3 cells were cultured in DMEM medium with 10% fetal bovine serum (FBS) and 1% penicillin/streptomycin at 37°C with 5% $CO_2$. Every 2-3 days, cells were passaged using trypsin.

## METHOD DETAILS

### Genetic analysis

Whole-exome sequencing and variant analysis were conducted by Beijing Youle Genomics Technology Company. The patient's peripheral blood was collected for DNA extraction, and a truseq DNA sample preparation kit was exploited for construct the DNA library. Subsequently, exon regions were captured using the Euler genomics exome capture V1 probe kit and high-throughput sequencing was performed using the illumina platform. Polyphen2_HVAR and SIFT were used to estimate the harmfulness of variants. The criteria for screening Candidate

mutations were as follows: (1) a minor allele frequency (<1%) in four public databases (the 1000 Genomes database, the Exome Aggregation Consortium (ExAC) Browser, the genome Aggregation Database (gnomAD) and Economy Prediction System (EPS)); (2) exonic nonsynonymous or splice site variants, or frameshift insertions/deletions (INDELs); (3) Genes associated with oocyte and early embryo development. The candidate gene was further confirmed by Sanger sequencing of the patient and her family members.

### Preparation of $Zp2^{T541M}$ mice

*Zp2* is located on the reverse strand of chromosome 7 in mouse genome. *Zp2* c.1622-1623CT >TG ($Zp2^{T541M}$) mutant mice were generated by CRISPR/Cas9, with B6D2F1 background. The *Zp2*-specific sgRNA mediated Cas9 nuclease spliceosome generated specific DNA double-strand breaks near the mutation sites, and single stranded DNA (ssDNA) containing the mutation nucleotides was used as the targeting vector for homologous recombination to achieve the site-specific mutation of *Zp2*. The sgRNA, Cas9 mRNA and targeting vector were co-injected into fertilized eggs and then embryos were transferred into foster mothers to produce $Zp2^{T541M}$ and $Zp2^{WT/T541M}$ mice. Genotyping was identified by Sanger sequencing.

### Fertility test and superovulation

For fertility test, 7-week-old $Zp2^{WT}$, $Zp2^{WT/T541M}$ and $Zp2^{T541M}$ female mice were mated continuously with fertile wild-type males for six months. The numbers of pups per female were recorded at birth.

To obtain MII oocytes, mice were injected intraperitoneally 10 IU of pregnant mare serum gonadotropin (PMSG) followed 48 hours later by 10 IU of human chorionic gonadotropin (hCG). 12-14 h after hCG injection, the superovulation-treated mice were killed and COCs were recovered from the oviductal ampulla. MII oocytes were harvested after short treatment of COCs with hyaluronidase (0.3 mg/ml) in M2 medium.

### Histological analysis and quantification of ovarian follicles

Mouse ovaries were collected and fixed in 4% paraformaldehyde (PFA) at 4°C overnight. Next, the ovaries underwent graded ethanol dehydration and paraffin embedding. Paraffin-embedded ovaries were continuously sectioned by 8 μm thickness. Every fifth section was selected and patched onto adherent slides for H&E staining. The sections were observed and imaged under a Leica Aperio VESA8 microscope. Ovarian follicles were classified as primordial follicles, primary follicles, secondary follicles and tertiary follicles based on accepted standards.[50] The counting principle was that only follicles with visible oocyte nucleuses were marked, and cumulative follicles counts was multiplied by 5 to get the final follicle numbers.

We performed PAS staining experiments using PAS stain kit. Briefly, after dewaxing and hydration, ovarian sections were treated with oxidant for 5-10 min, rinsed with water for 5 min, then stained with Schiff reagent for 10-15 min and washed for 5 min. The samples were counterstained with hematoxylin and imaged with Leica Aperio VESA8 microscope.

### Immunofluorescent staining

Paraffin-embedded ovarian sections were treated by deparaffinization, stepwise rehydration through an ethanol series (100, 95, 90, 80, 70% ethanol) and antigen retrieval with heated 10 mM sodium citrate solution. After washing with phosphate-buffered saline (PBS) three times, sections were blocked with 5% bovine serum albumin (BSA) in PBS 1 h at room temperature and incubated with anti-ZP2 primary antibody (1:1000 dilution) overnight at 4°C. Next day, sections were incubated with secondary antibody at room temperature for 1 h, washed three times with PBS, stained with 4′,6-diamidino-2-phenylindole (DAPI) for 10 min and mounted. Images were observed and scanned using confocal lasers scanning microscope (Zeiss LSM 880).

Apoptosis of the follicles was detected by a terminal deoxynucleotidyl transferase 2′-deoxyuridine, 5′-triphosphate nick end labeling (TUNEL) assay using DeadEnd™ Fluorometric TUNEL System, according to manufacturer's instructions.

To visualize the TZPs, phalloidin staining was conducted. Ovaries were frozen using liquid nitrogen and sectioned at 10 μm thickness. After permeabilisation, fixation and blocking, the slices were incubated with Alexa Fluor™ 466 Phalloidin (1:200 dilution) overnight at 4°C. After washing with PBS, the slices were stained with DAPI for 10 min, mounted and imaged using confocal lasers scanning microscope (Zeiss LSM 880).

### Plasmids construction

The cDNA encoding mouse ZP2 open reading frame (ORF) was amplified and the resulting PCR product was recombined with eukaryotic expression vector pcDNA3.1 plasmid. MCY-tag was fused to N-termini of ZP2. Human $ZP2^{WT}$ plasmid was acquired from plasmid bank in our laboratory. Site-specific mutations were introduced to $Zp2^{WT}$ and $ZP2^{WT}$ plasmids using KOD-Plus-Mutagenesis Kit to introduce $Zp2^{T541M}$ and $ZP2^{T539M}$ plasmids, respectively.

### Cell transfection

Transient transfections were carried out using Lipofectamine 3000 when cells were 70-80% confluent. Before transfection, cells were washed with PBS and maintained in DMEM medium without serum. For each 6cm dish, 4 μg DNA plasmid and 8 μl P3000 reagent were diluted into 250 μl opti-MEM medium. Then diluted DNA was mixed with diluted Lipofectamin 3000 to form the transfection complex. After incubation at

room temperature for 15 min, the transfection complex was added to cells. Transfected cells were collected for immunofluorescent staining after 24 h and for western blotting after 48 h.

### Western blotting

48 h after transfections, supernatants were collected, centrifuged (4°C, 500g, 5 min) to discard cell debris, and concentrated using Amicon Ultra-4 centrifugal filter devices in accordance with the manufacturer's protocol. Cells were collected, lysed by RIPA lysis buffer supplemented with protease inhibitor cocktail (PIC), incubated for 30 min on ice, then centrifuged at 15,000 g for 20 min at 4°C to discard cell debris. Both supernatants and cell lysates were quantified by BCA protein assay kit and boiled for 5 min with 5×loading buffer. Different proteins were separated by 10% sodiumdodecyl sulfate polyacrylamide gel electrophoresis (SDS-PAGE) and transferred to polyvinylidene fluoride (PVDF) membranes. After blocking with 5% BSA in TBST (tris buffered saline with 0.1% tween 20) at room temperature for 1 h, membranes were incubated with antibodies to ZP2 (1:1000 dilution), MYC (1:2000 dilution), and β-actin (1:1000 dilution). Next day, membranes were washed three times with PBS before being incubated with secondary antibodies for 1 h at room temperature, and then washed again with PBS. The secondary antibodies used were horseradish peroxidase conjugated Goat Anti-Rat IgG (1:3000 dilution), Goat Anti-Rabbit IgG (1:3000 dilution) and Goat Anti-Mouse IgG (1:3000 dilution). Signals were detected with enhanced chemiluminescence detection system.

## QUANTIFICATION AND STATISTICAL ANALYSIS

All experiments were repeated at least three times. Data were presented as mean ± SEM. One-way ANOVA test was used for statistical analysis between the $Zp2^{WT}$, $Zp2^{WT/T541M}$ and $Zp2^{T541M}$ groups using GraphPad Prism 8. $P < 0.05$ was considered as a significance level.